



ELSEVIER

Journal of Chromatography A, 887 (2000) 421–437

JOURNAL OF
CHROMATOGRAPHY A

www.elsevier.com/locate/chroma

Chiral anion exchangers applied to capillary electrochromatography enantioseparation of oppositely charged chiral analytes: investigation of stationary and mobile phase parameters

Michael Lämmerhofer*, Ernst Tobler, Wolfgang Lindner

Institute of Analytical Chemistry, University of Vienna, Währingerstrasse 38, A-1090 Vienna, Austria

Abstract

Weak anion-exchange (WAX) type chiral stationary phases (CSPs) based on *tert.*-butyl carbamoyl quinine as chiral selector (SO) and different types of silica particles (porous and non-porous) as chromatographic support are evaluated in packed capillary electrochromatography (CEC). Their ability to resolve the enantiomers of negatively charged chiral analytes, e.g., *N*-derivatized amino acids, in the anion-exchange mode and their electrochromatographic characteristics are described in dependence of several mobile phase parameters (pH, buffer type and concentration, organic modifier type and concentration) and other experimental variables (electric field strength, capillary temperature). The inherent “zwitterionic” surface character of such silica-based WAX type CSPs (positively charged SO and negatively charged residual silanols) allows the reversal of the electroosmotic flow (EOF) towards the anode at pH values below the isoelectric point (*pI*) of the modified surface, whereas a cathodic EOF results at pH values above the *pI*. Since for negatively charged analytes also an electrophoretic transport increment has to be considered, which can be either in or against the EOF direction, several distinct modes of elution have been observed under different stationary phase and mobile phase conditions: (i) co-electrophoretic elution of the negatively charged solutes with the anodic EOF in the negative polarity mode, (ii) counter-electrophoretic elution with the cathodic EOF in the positive polarity mode, and (iii) electrophoretically dominated elution in the negative polarity mode with a cathodic EOF directed to the injection end of the capillary. Useful enantioseparations of chiral acids have been obtained with all three modes. Enantioselectivity values as high as under pressure-driven conditions and theoretical plate numbers up to 120 000 per meter could be achieved under electrically driven conditions. A repeatability study yielded RSD values below 2% for retention times and RSD values in the range of 5–10% for theoretical plate numbers and resolution, thus clearly establishing the reliability of the investigated anion-exchange type CEC enantioseparation methods. © 2000 Elsevier Science B.V. All rights reserved.

Keywords: Enantiomer separation; Chiral stationary phases, CEC; Mobile phase composition; Electrochromatography

1. Introduction

Currently, many research activities in the field of

capillary electrochromatography (CEC) focus on the re-development of liquid chromatographic separations under electrically driven conditions. This also holds true for chiral separations. Thus, several CEC enantioseparation methods have been presented (i) using chiral selectors (SOs) as mobile phase additives in combination with capillaries packed with achiral stationary phases [1–6], or (ii) using capil-

*Corresponding author. Tel.: +43-1-4277-52323; fax: +43-1-4277-3151826.

E-mail address: michael.laemmerhofer@univie.ac.at (M. Lämmerhofer)

laries packed with chirally modified particles or filled with monolithic chiral stationary phases (CSPs) and achiral mobile phases. A wide variety of chiral packings have already been investigated for CEC application, including protein type CSPs [7,8] cyclodextrin-based CSPs [1,9,10], “Pirkle-concept” CSPs [11], vancomycin bonded phases [12], poly-*N*-acryloyl-*L*-phenylalanine ethylester- and cellulose tris-(3,5-dimethylphenylcarbamate)-based CSPs [13]. Besides, molecular imprinted polymers (MIPs) have also been used as CSPs either in particulate form [14,15] or as monoliths directly prepared in the capillary [16–18]. In another approach, monolithic capillary columns have been prepared by in situ copolymerization of a methacrylate-type chiral monomer, functionalized with (*S*)-valine-3,5-dimethylanilide, in presence of cross-linker, chargeable co-monomer, and porogenic solvents within a fused-silica capillary [18].

Recently, we could demonstrate that the enantiomers of negatively charged chiral analytes can be separated by CEC methods involving ion-pair [6] and anion-exchange [19] selectivity principles employing quinine-derived SOs. In this study, the effect of the chromatographic support material of quinine carbamate-based chiral anion exchangers, which have been prepared by carrying out the same surface modification protocol with different silica particles, is investigated. Thus, three different types of silica particles have been used for the immobilization of the positively chargeable *tert*-butyl carbamoyl quinine SO, which (i) provides the chromatographic selectivity being responsible for chiral discrimination and separation of the enantiomers of the analyte (selectand, SA) by an anion-exchange mechanism, and (ii) in the CEC mode modulates or determines the electroosmotic flow (EOF) of the CSP. The chiral packings based on porous Kromasil 100, 5 μm particles (CSP A) [20,21] and Hypersil 120, 3 μm (CSP B) have due to their large specific surface areas accessible for modification a high molar SO loading (CSP A: 270 $\mu\text{mol/g}$ corresponding to 0.8 $\mu\text{mol/m}^2$; CSP B: 160 $\mu\text{mol/g}$ or 0.9 $\mu\text{mol/m}^2$). CSP C is based on non-porous Micra NPS, 1.5 μm particles as support material. Selection of this type of silica was primarily guided by considerations that the small surface area ($<3 \text{ m}^2/\text{g}$) will result in low SO loading ($\sim 9 \mu\text{mol/g}$) yielding very short run times;

high-performance liquid chromatography (HPLC) evaluation of this chiral packing material was found to be quite promising enabling high-speed enantio-separations of chiral acids within 2–3 min [22,23].

In the usual working pH range of these weak anion-exchange (WAX) type CSPs [20,24] between pH 5 and 7 the basic tertiary amine of the quinuclidine moiety is protonated and positively charged, while the residual silanols of the chirally modified silica surface will be negatively charged yielding a “zwitterionic” surface. As a result of the amphoteric character of the surface, the electroosmotic flow may be directed either to the cathode [at pH values of the mobile phase above the apparent isoelectric point (*pI*) of the surface] or to the anode (below the *pI*).

For the anion-exchange type process, the analytes have to be negatively charged, so that also the anodically directed electrophoretic transport increment has to be considered. Overall, the transport of the negatively charged solute species through the capillary column may either be electroosmotically or electrophoretically dominated, i.e., one of the two transport processes, which may have opposite signs or directions, is of larger numerical value.

Accordingly, in the discussion of the presently investigated silica-based WAX type CEC systems with negatively charged analytes will be distinguished between three different elution modes: (i) co-electrophoretic elution with the anodic EOF in the negative polarity mode: either electroosmotically or electrophoretically dominated, (ii) electroosmotically dominated counter-electrophoretic elution with the cathodic EOF in the positive polarity mode, (iii) electrophoretically dominated elution in the negative polarity mode, while the EOF is cathodic and thus directed towards the injection end of the capillary.

Which of these modes is observed experimentally will strongly depend on stationary and mobile phase parameters.

In this context, it should be emphasized that enantioselectivity is exclusively related to the chromatographic process, i.e., the affinity type anion-exchange process. The SA enantiomers will solely be separated if they interact with the SO moiety with different binding strength. Thereby, SO–SA interaction is primarily driven by ionic interaction between the negatively charged SAs and the positively charged SO moiety. In addition, other non-covalent

attractive and/or repulsive interactions (e.g., hydrogen bonding between the carbamate group of the SO and complementary binding sites in the SAs, π – π interaction between the quinoline– π -base of the SO and complementary aromatic groups of the SAs) come into play and support or trigger discrimination between SA enantiomers [25,26].

The aims of this study can be summarized as follows: (i) the chromatographic and electroosmotic properties of CSPs A–C should be characterized pointing out the effect of the support material. Thereby, the influence of several experimental variables (pH, organic modifier type and concentration, buffer type and concentration, temperature, electric field strength) will be shown. (ii) The relative influence of the various processes involved should be

estimated. (iii) It should be clarified which of the above proposed elution modes is most favorable for CEC enantioseparation of negatively charged chiral analytes on chiral anion exchangers.

2. Experimental

2.1. Materials

CSPs A–C (see Fig. 1) were prepared by a standard procedure that is described in detail elsewhere [24,27].

First, thiol functionalized silica was prepared by refluxing a suspension of the respective silica particles and 3-thiopropyl trimethoxy silane (Aldrich) in

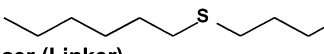
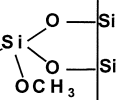
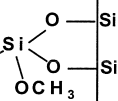
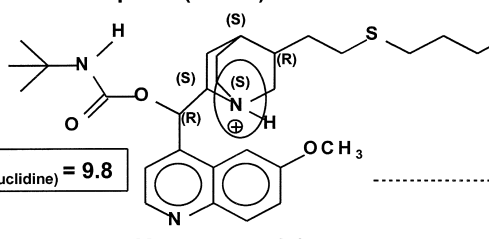
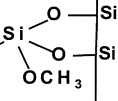
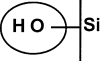
Surface modification			Chromatographic support: porous or non-porous silica	
End-Capping + Spacer (Linker) 				CSP A: Kromasil 100-5μm
Spacer (Linker) $pK_{a(\text{thiol})} \sim 10$				Surface area: 340 m ² /g CSP B: Hypersil 120-3μm
Selector + Spacer (Linker) $pK_{a2(\text{quinuclidine})} = 9.8$ $pK_{a1(\text{quinoline})} = 3.9$ 				Surface area: 170 m ² /g CSP C: Micra NPS-1.5μm Surface area: < 3 m ² /g
				Residual silanols $pK_{a(\text{silica})} = 2 - 4$
Variables:	CSP	SO-coverage $\mu\text{mol/g}$ $\mu\text{mol/m}^2$	Variables: silanol activity porosity and pore size specific surface area particle diameter	
	A	270 0.8		
	B	160 0.9		
	C	~ 9 ~ 3		

Fig. 1. Structures of weak anion-exchange (WAX) type chiral stationary phases (CSP A–C) investigated in this study and CSP parameters relevant for their electrochromatographic characteristics.

toluene (analytical-reagent grade); for CSP A Kromasil 100, 5 μm (Eka, Bohus, Sweden), for CSP B Hypersil 120, 3 μm (Hypersil, purchased from HPLC Service, Breitenfurt, Austria), and for CSP C Micra NPS, 1.5 μm (Micra Scientific, purchased from Bischoff Chromatography, Leonberg, Germany) were used as chromatographic support materials. The elemental analyses of the resulting thiol modified silica particles yielded the following results: A: 4.58% C, 1.12% H; this corresponds to 0.8–0.9 mmol thiol groups per g silica. B: 2.95% C, 0.61% H (0.5–0.6 mmol thiol groups per g silica). C: 0.48% C, 0.87% H (0.08–0.10 mmol thiol groups per g silica).

Subsequently, the corresponding silica particles with reactive thiol groups were employed for immobilization of *tert*-butyl carbamoyl quinine [27] by a radical addition reaction in chloroform. Elemental analyses yielded the following results: CSP A: 12.7% C, 1.89% H, 1.25% N; this corresponds to a calculated SO loading of 0.27 mmol/g silica. CSP B: 7.59% C, 1.13% H, 0.66% N (corresponding to a SO loading of 0.16 mmol/g silica), and CSP C: 0.74% C, 0.93% H, (% N not determined; the calculated SO loading of this CSP is about 9 $\mu\text{mol/g}$ silica).

In a final end-capping step some of the remaining thiol groups have been modified with hexyl groups by a radical addition reaction with 1-hexene. The results of the elemental analyses after end-capping were as follows: CSP A: 13.27% C, 1.97% H; CSP B: 8.19% C, 1.20% H; CSP C: no significant change of atom loading was observable.

The chirally modified silica particles were packed to a length of 250 mm into fused-silica capillaries of 75 μm (CSP A) and 100 μm I.D. (CSPs B and C), respectively, either by electrokinetic (CSP A) or high-pressure (CSPs B and C) slurry packing procedures, respectively. The total length (L_{tot}) of the capillary columns was 335 mm each. A detection window was fabricated by cutting off the polyimide coating close to the end frit ($L_{\text{eff}}=250$ mm). The CEC Hypersil 120, 3 μm C_{18} capillary column, 335 (250) \times 0.1 mm I.D., was purchased from Hewlett-Packard (Waldbronn, Germany). For the HPLC experiments, a column of 150 \times 4.6 mm I.D. packed with CSP A was utilized. CE experiments were carried out with a 100 μm I.D. bare fused-silica capillary (Composite Metal Services, Worcestershire,

UK) of the same geometry as packed columns ($L_{\text{tot}}=335$ mm, $L_{\text{eff}}=250$ mm) under otherwise identical conditions as in the corresponding CEC experiments.

N-(3,5-Dinitrobenzyloxycarbonyl) leucine (DNZ-Leu) and *N*-(2,4-dinitrophenyl) valine (DNP-Val) were prepared by derivatization of the respective amino acids with 3,5-dinitrobenzyl chloroformate (prepared from phosgen and 3,5-dinitrobenzyl alcohol; both from Fluka) and Sangers reagent (2,4-dinitrofluorobenzene; Aldrich), respectively, following standard derivatization protocols [23,28]. All other racemic chiral analytes as well as enantiomers thereof were purchased from Bachem (Bubendorf, Switzerland), Aldrich and Sigma, respectively.

Acetonitrile (ACN) and methanol (MeOH) were of HPLC-grade and supplied by J.T. Baker. 2-(*N*-Morpholino)ethanesulfonic acid (MES) was provided by Sigma. 4-(2-Hydroxyethyl)-piperazin-1-ethanesulfonic acid (HEPES), glacial acetic acid (AcOH) and triethylamine (NEt_3) were from Fluka. Sodium phosphate was supplied by Merck (Darmstadt, Germany).

The pH of the mobile phases was measured in the aqueous–organic mixture and thus refers to the apparent pH (pH_a). The mobile phases were filtered through a 0.2- μm nylon membrane filter and degassed by sonication prior use.

2.2. Instrumentation

A Hewlett-Packard HP 3D capillary electrophoresis (CE) system with an external pressurization system and HP 3D-CE chemstation software was used to perform the CEC runs. Throughout the study an external pressure of 8 bar was applied to both ends of the capillary and buffer vials, respectively. The samples (0.5 mg/ml) were injected electrokinetically.

3. Results and discussion

3.1. Influence of mobile phase pH on EOF

As already discussed, CSPs A–C are based on different chromatographic supports; as a consequence SO coverages (see Fig. 1) as well as silanol activities, which determine the EOF behavior of

these CSPs, vary considerably. Due to the “zwitterionic” surface character, magnitude and direction of the EOF are strongly depending on the mobile phase pH, as is shown in Fig. 2. Considering the pH curve of CSP A (porous support and high SO coverage) obtained with methanol as organic modifier, at pH values above 6.3 the EOF is directed towards the cathode. On the other hand, at pH values below 6.3 an anodic EOF is observed indicating a positive net charge and ζ potential of the modified surface. This curve is shifted with acetonitrile so that the isoelectric point is apparently located at higher pH values; consequently, an anodic EOF is observed over a wider pH range. This is illustrated in Fig. 2 for CSP B, which has also a high SO coverage. In contrast, on CSP C (non-porous silica particles with low SO loading) a cathodic EOF is obtained almost over the entire pH range studied. Obviously, this CSP has high silanol activity leading to an excess of negative charge on the surface at $\text{pH}_{\text{app}} > 3.7$. For sake of comparison, the pH curve obtained with a conventional reversed-phase type stationary phase (CEC Hypersil 120, 3 μm C₁₈) is also shown. As

expected this stationary phase provided a cathodic flow throughout the investigated pH range.

3.2. Influence of mobile phase pH on chromatographic and electrophoretic parameters

Via the mobile phase pH the potential and actual capacity of the chiral anion exchangers is controlled, determining not only EOF characteristics, but having also a significant effect on the chromatographic properties of the stationary phase. In addition, effective electrophoretic mobility is considerably affected so that the mobile phase pH is estimated to be the key parameter to control the several processes and to optimize CEC enantioseparations on the chiral anion exchangers under study. Regarding the separation of Fmoc-Leu on WAX type CSP B (see Fig. 3a) effective retention factors show a maximum that is located at mobile phase pH of 5.5. This behavior compares fairly well with that of LC [20,24], indicating the dominance of the chromatographic process in the usual working pH range between 4 and 6. In this

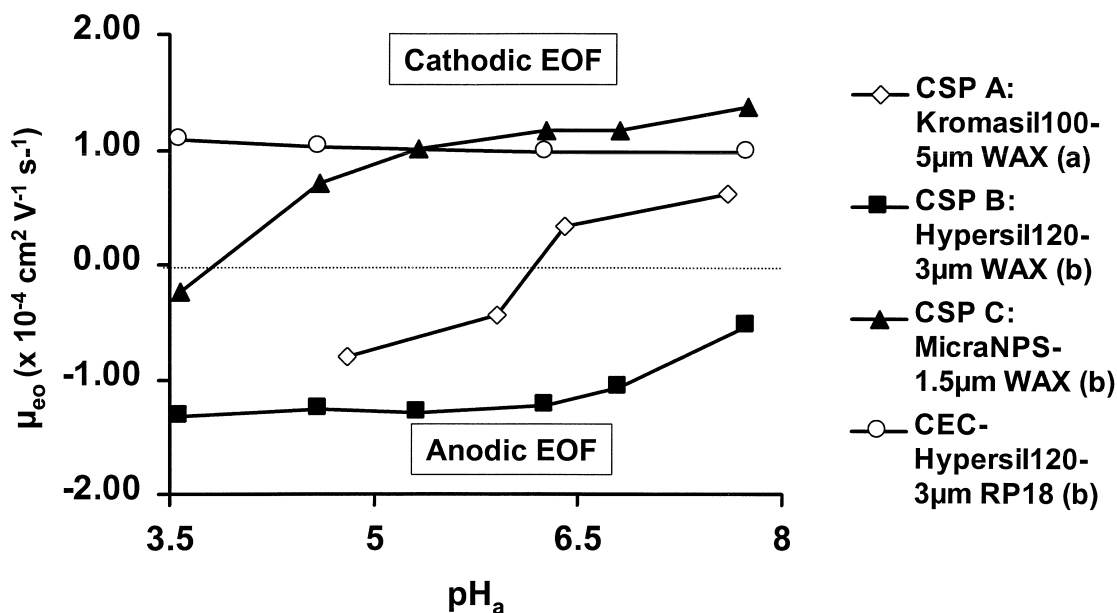


Fig. 2. Influence of mobile phase pH (apparent pH, pH_a) on electroosmotic mobility (μ_{eo}) on WAX type CSPs A–C (see Fig. 1). For sake of comparison also the EOF characteristics of a reversed-phase type CEC capillary column are depicted in the plot. CEC conditions: EOF marker: thiourea; T : 20°C; voltage: ± 15 kV; injection: ± 5 kV/5 s; detection: UV at 250 nm; mobile phase: (a) MeOH–10 mM CH_3COOH (80:20) (pH_a adjusted with NET_3); (b) acetonitrile–100 mM MES (80:20) (pH_a adjusted with NET_3).

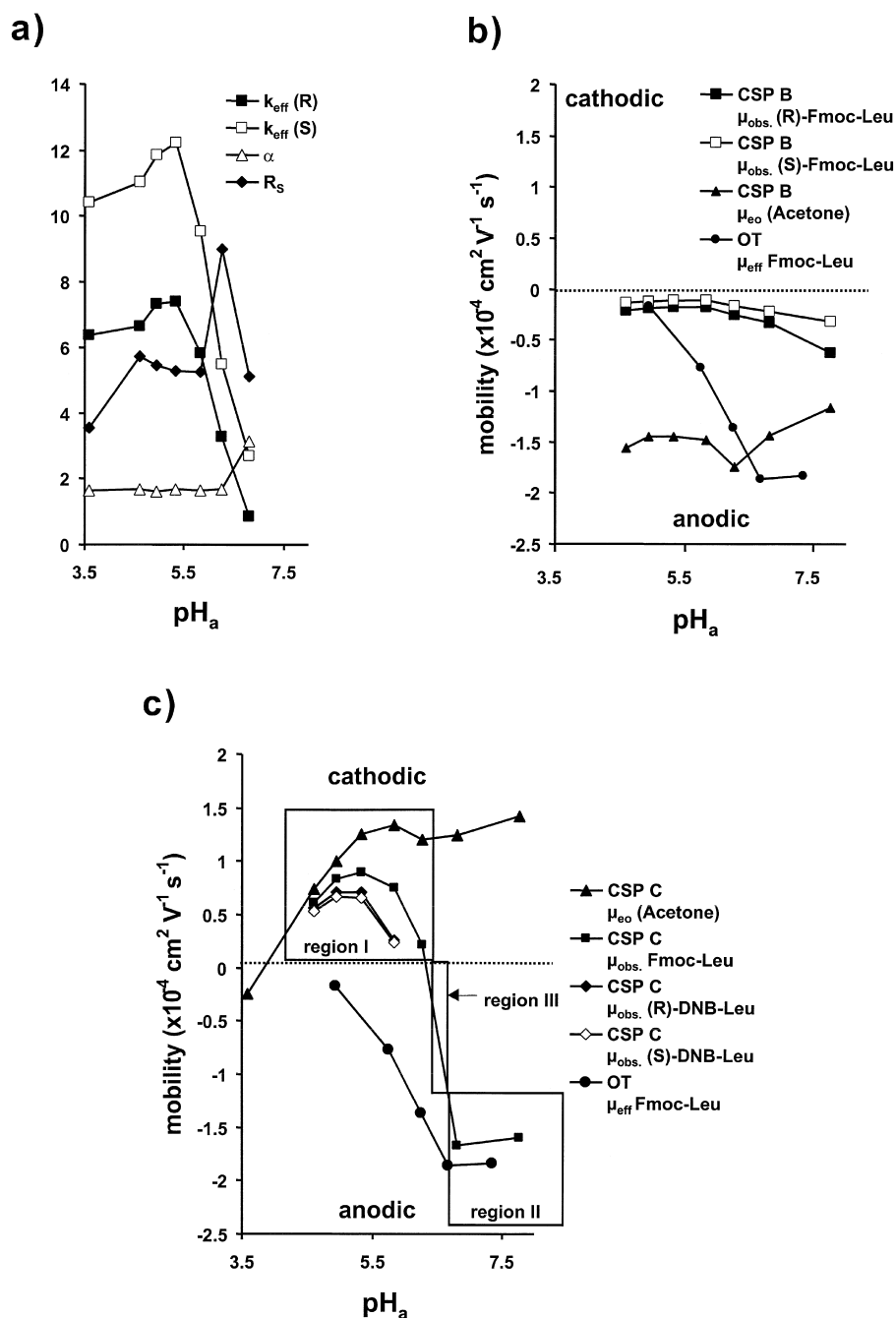


Fig. 3. Influence of mobile phase pH (pH_a): (a) on the effective chromatographic parameters of (R,S)-Fmoc-Leu enantioseparation on WAX type CSP B; (b) on observed mobilities ($\mu_{\text{obs.}}$) of Fmoc-Leu and on the eluent mobility (μ_{eo}) on WAX type CSP B, and (c) on μ_{eo} as well as on $\mu_{\text{obs.}}$ of Fmoc-Leu and DNB-Leu enantiomers on WAX type CSP C. In addition, effective electrophoretic mobility (μ_{ep}) in an open bare fused-silica capillary (OT) in dependence of mobile phase pH is also shown. Experimental conditions: mobile phase: acetonitrile–100 mM MES (80:20) (pH_a adjusted with NET_3); T : 20°C; voltage: ± 15 kV; injection: ± 15 kV/10 s; detection: UV at 250 nm.

pH range rather constant EOF (μ_{eo}) is obtained (see Fig. 3b). At higher pH values, the electrophoretic transport process gains on influence, while EOF only slightly decreases at a pH above 6.5. Simultaneously, the actual ion-exchange capacity decreases leading to enhanced observed mobilities of (*R*)- and (*S*)-Fmoc-Leu enantiomers (see Fig. 3b). In the entire pH range investigated the analytes eluted in the negative polarity mode (see Fig. 3b). In LC optimal enantioselectivity is yielded at pH values below 6. In CEC, optimum enantioselectivity is observed at higher pH (see Fig. 3a). This modulation can be attributed to the influence of the electrophoretic process. Optimal resolution has been observed at pH_a 6.3, however, in terms of robustness operation at pH_a values between 5 and 6 is recommended (see Fig. 3a).

The pH dependence on non-porous CSP C, where due to the small surface area and low SO loading the chromatographic increment is much smaller compared to CSP B, is depicted in Fig. 3c). In the pH range between 4.5 and 6.3 (region I) (see Fig. 3c) the Fmoc-Leu enantiomers elute in the positive polarity mode. Obviously, the cathodic EOF is dominating the overall transport of the analytes through the capillary column, while oppositely directed electrophoretic migration is smaller in its magnitude (see Fig. 3c). Due to low SO loading of CSP C the Fmoc-Leu enantiomers have not been separated under the given conditions; nevertheless, it should be pointed out that between pH 5.3 and 4.6 peak efficiencies were quite high with theoretical plate numbers between 120 000 and 160 000 per meter. In contrast, DNB-Leu enantiomers, which have higher affinity to the SO than Fmoc-Leu and therefore lower observed mobilities, are well separated on CSP C in the pH range between 4.5 and 6. At pH values above 6.8 (indicated as region II) the electrophoretic migration becomes the driving force for elution of Fmoc-Leu on CSP C; the analytes are eluted in the negative polarity mode, while the EOF is directed towards the cathode at the injection end of the capillary. In the small pH band between 6.3 and 6.8 (region III) instabilities (peak splitting with extraordinarily sharp peaks) have been observed in the analysis of Fmoc-Leu on CSP C (also on CSP B similar observations and instabilities have been observed at pH values near the apparent pI of the CSP).

3.3. Comparison of various modes of elution

In Fig. 4 the separations of DNZ-Leu enantiomers that have been achieved at pH_a 6 on the three different WAX type CSPs A–C are compared. The enantiomers of DNZ-Leu are separated with high enantioselectivity values on both porous WAX type CSPs A and B (CSP A: $\alpha=2.16$; CSP B: $\alpha=2.48$) in the negative polarity mode (co-electrophoretic elution with anodic EOF). Reasonable efficiencies with theoretical plate numbers up to 120 000 per meter for the first eluting enantiomer have been achieved. However, the separations suffer from the long run times, which are a result of high SO loadings, strong ionic SO–SA interactions, low flow-rates (caused by the high buffer concentrations that have to be used to weaken the strong ionic interactions) and low electric field strengths (which are favorable with regard to system stability and efficiency). In contrast, the enantiodiscrimination capability of the non-porous WAX type CSP C for DNZ-Leu is rather poor compared to the porous analogs. Under the given conditions the SA is eluted in the positive polarity mode (cathodic EOF). It seems that this counter-electrophoretic elution mode yields less efficient peak performance compared to the co-electrophoretic elution mode.

However, other SAs can be nicely separated on non-porous WAX type CSP C, e.g., DNB-Leu (see Fig. 5). With different organic modifiers the analytes are either eluted in the positive polarity mode, i.e., overall transport is electroosmotically dominated (see Fig. 5a) (this mode is observed with ACN as organic modifier which yields higher flow-rates than methanol), or in the negative polarity mode, i.e., overall transport is electrophoretically dominated (see Fig. 5b) (due to low EOF of methanol).

Other successful enantioseparations on WAX type CSPs B and C are summarized in Table 1. Generally, it appears that SAs which have been successfully separated on quinine carbamate-based anion exchangers by HPLC can also be separated by CEC. As these chiral anion exchangers are typically operated in the hydro–organic (reversed-phase) mode, their enantiodiscrimination capability is maintained in CEC, however, some modulation of enantioselectivity and retention behavior can be expected due to

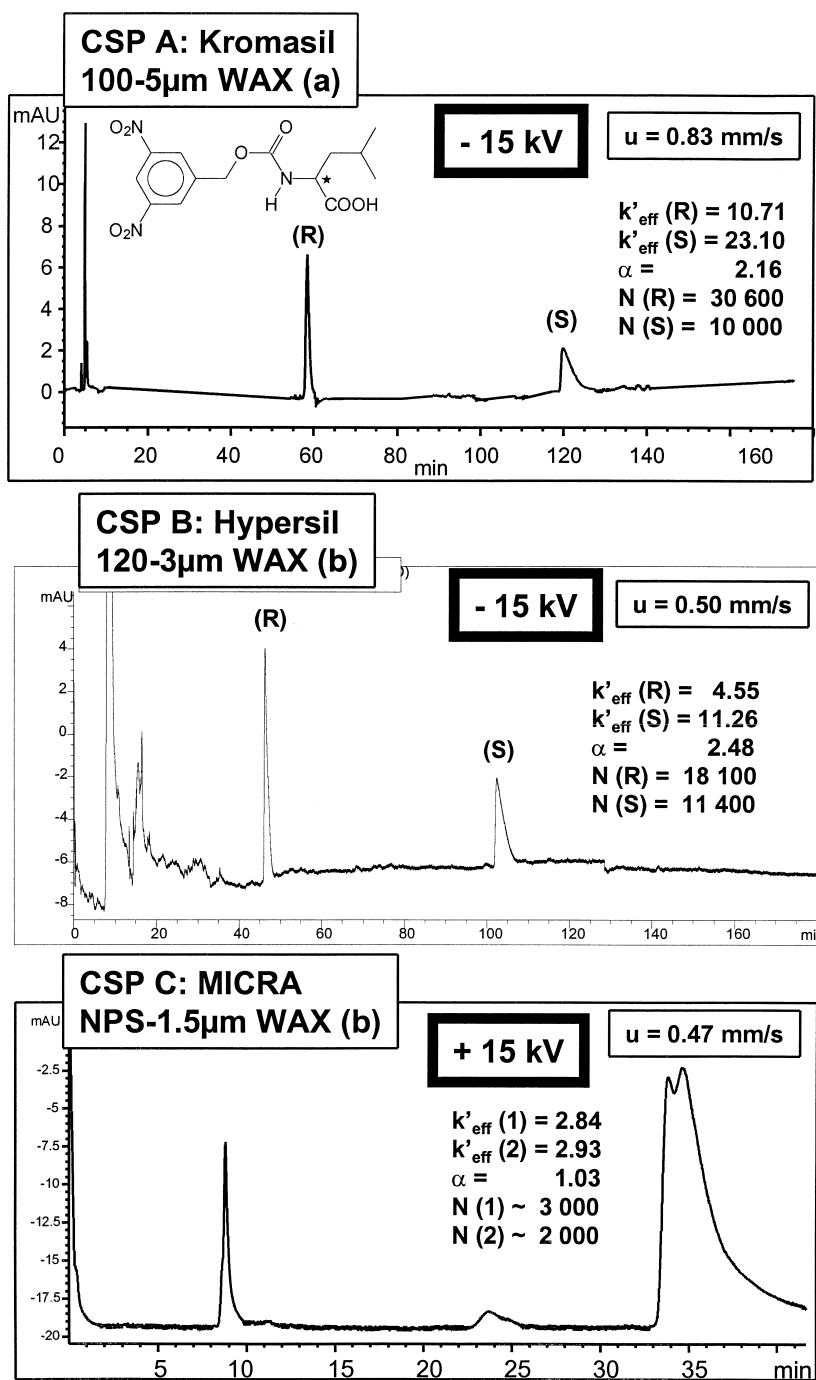


Fig. 4. CEC separations of DNZ-Leu enantiomers on WAX type CSPs A–C (see Fig. 1). Experimental conditions: T : 20°C; detection: UV at 250 nm; voltage: ± 15 kV; injection: -15 kV/10 s (CSPs A, B) and $+10$ kV/5 s (CSP C), respectively; mobile phase: (a) ACN–50 mM NEt_3HAc (80:20) ($\text{pH}_a=6.0$; adjusted with NEt_3); (b) ACN–100 mM MES (80:20) ($\text{pH}_a=6.0$; adjusted with NEt_3).

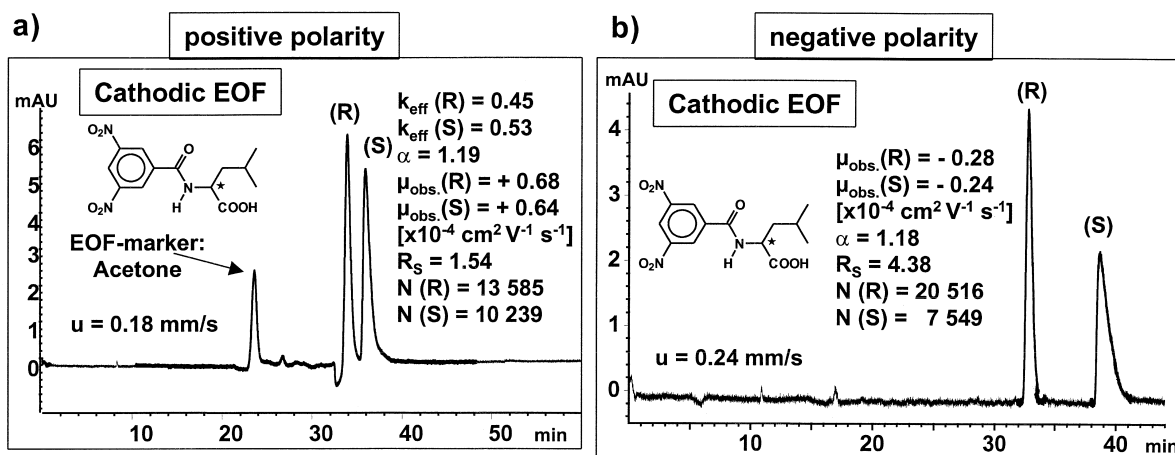


Fig. 5. DNB-Leu enantioseparations on WAX type CSP C: (a) electroosmotically vs. (b) electrophoretically dominated elution mode. Experimental conditions: mobile phase: organic modifier–0.1 M MES (80:20); $\text{pH}_a = 6.0$ (adjusted with NET_3); (a) organic modifier: ACN; (b) organic modifier: MeOH; voltage: (a) +6 kV (+0.37 μA); (b) –15 kV (–5 μA); injection: $\pm 10 \text{ kV}/5 \text{ s}$; T : 20°C; detection: UV at 250 nm.

Table 1
CEC enantioseparations on WAX type CSPs B and C (T : 20°C)

SA ^a	CSP	Mobile phase ^b	Voltage (kV)	I (μA)	$k_{\text{eff}}(1)$	$k_{\text{eff}}(2)$	e.o. ^c	α	$\mu_{\text{obs.}}(1)$ ($\cdot 10^{-4} \text{ cm}^2 \text{ V}^{-1} \text{ s}^{-1}$)	$\mu_{\text{obs.}}(2)$ ($\cdot 10^{-4} \text{ cm}^2 \text{ V}^{-1} \text{ s}^{-1}$)	R_S	$N(1)$	$N(2)$
DNZ-leucine	B	a	–15	–3.2	4.81	11.63	R	2.42	–0.189	–0.087	22.41	19 053	13 053
Fmoc-leucine	B	b	–15	–11.0	3.65	6.16	R	1.69	–0.334	–0.217	16.21	23 660	22 766
1,1'-Binaphthyl-2,2'-diyl hydrogenphosphate	B	b	–15	–11.0	6.65	10.33	R	1.55	–0.209	–0.141	7.36	6861	5141
Bz-leucine	B	c	–15	–8.5	2.67	5.61	R	2.10	–0.416	–0.231	11.40	11 112	4884
DNP-valine	B	d	–15	–6.6	3.21	4.25	S	1.32	–0.375	–0.300	6.41	17 800	11 215
DNB-leucine	C	e	6	0.4	0.44	0.52	R	1.19	0.687	0.649	1.63	15 557	10 799
DNB-leucine	C	d	–25	–10.3	–	–	R	1.14	–0.275	–0.240	4.32	29 851	11 185
Fmoc-arginine	B	d	–25	–10.9	3.96	6.39	R	1.61	–0.107	–0.072	9.82	9895	9934
Fmoc-leucine	B	d	–25	–9.6	2.61	5.29	R	2.02	–0.183	–0.105	11.28	11 365	5490
Fmoc-phenylalanine	B	d	–20	–6.8	3.94	6.35	R	1.61	–0.108	–0.073	8.82	11 353	6587
Fmoc-tryptophan	B	d	–20	–7.1	10.74	16.40	R	1.53	–0.054	–0.036	7.33	8454	4484
Fmoc-asparagin	B	d	–20	–7.4	2.23	3.05	R	1.37	–0.175	–0.139	4.21	2784	11 793

^a DNZ: *N*-(3,5-dinitrobenzyloxycarbonyl); Fmoc: *N*-(9-fluorenylmethoxycarbonyl); Bz: *N*-benzoyl; DNP: *N*-(2,4-dinitrophenyl); DNB: *N*-(3,5-dinitrobenzoyl).

^b Organic modifier–buffer (80:20), organic modifier: a–e: ACN, f: MeOH; buffer: a: 75 mM MES ($\text{pH}_a = 6.0$; NET_3); b: 150 mM MES ($\text{pH}_a = 6.2$; NET_3); c: 150 mM MES ($\text{pH}_a = 6.0$; NET_3OH); d: 100 mM MES ($\text{pH}_a = 6.0$; NET_3); e: 100 mM MES ($\text{pH}_a = 5.0$; NET_3).

^c e.o.: Elution order: configuration of first eluted enantiomer.

the electrophoretic increment, in particular for multiple charged species. Other type of CSPs, as e.g., Pirkle-concept CSPs which are typically operated in the normal-phase mode, loose significantly in enantioselectivity by switching from non-aqueous HPLC to hydro-organic conditions in CEC [11]).

3.4. Influence of organic modifier content on EOF

The dependence of different organic modifier contents on eluent mobility has been studied for ACN and MeOH under otherwise identical conditions (see Fig. 6). Generally, the findings are in agreement with those observed in reversed-phase CEC employing C_{18} or strong cation-exchange (SCX) type stationary phases [29]. Acetonitrile gives greatly enhanced flow-rates compared to methanol, e.g., at a modifier content of 80% μ_{eo} is by a factor of about 2.8 higher for acetonitrile. While for the methanol system the eluent mobilities widely show the behavior expected from dielectric/viscosity ratios of MeOH–water (with minimum EOF rates around 60%), for the ACN–water system EOF steadily increases with increasing ACN content. This unexpected behavior for the ACN system has been

attributed by other authors to a simultaneous change of the ζ potential of the packing [30].

3.5. Influence of buffer concentration and buffer type

In accordance with the anion-exchange process the actual capacity of the anion exchanger and thus retention can be reduced by increasing the total buffer concentration, as illustrated in Fig. 7a) for a MES–buffer system. Simultaneously, enantioselectivity is more or less unaffected. Unfortunately, with the increase of the buffer concentration the EOF velocity decreases (see Fig. 7b) as a consequence of decreasing double layer thickness and ζ potential. On the other hand, high buffer concentrations may have a positive effect on system robustness; when charged sample components are injected.

We also investigated whether with other counterions stable conditions and enhanced elution strength can be afforded. The results of these experiments are illustrated in Table 2. It can be seen that peak efficiencies are greatly affected by the buffer type and can be improved by selection of a proper buffer system. The presented data also reveal that elution strength on the investigated WAX type CSPs de-

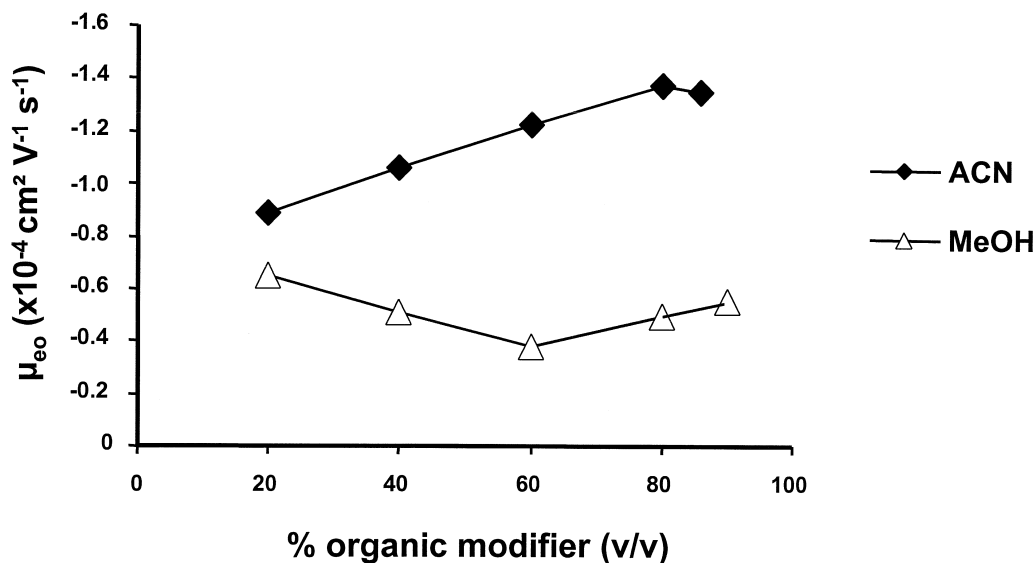


Fig. 6. Influence of organic modifier type and content on electroosmotic mobility (μ_{eo}). EOF marker: acetone. Experimental conditions: stationary phase: CSP B; mobile phase: organic modifier–MES buffer; total buffer concentration: 20 mM; $pH_a=6$, adjusted with NEt_3 ; T : 20°C; voltage: –20 kV; injection: –15 kV/10 s; detection: UV at 250 nm.

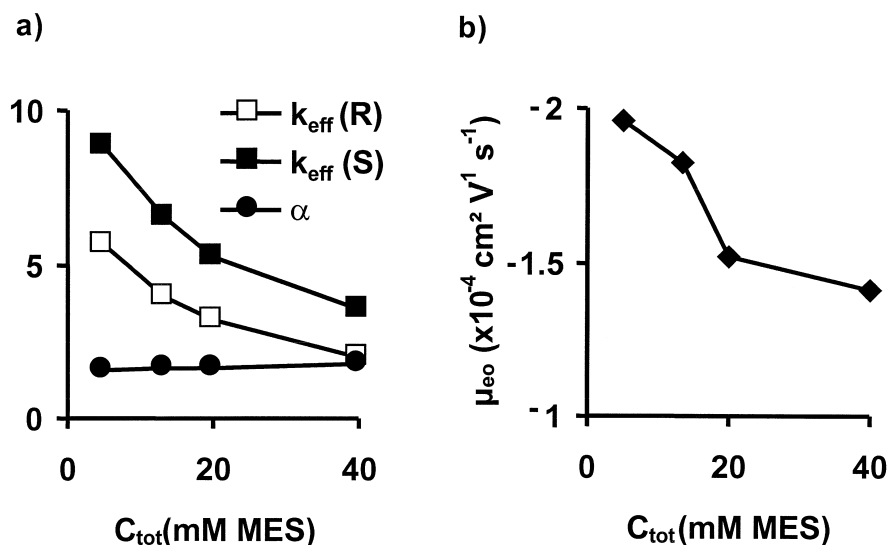


Fig. 7. Influence of total buffer concentration (C_{tot}) on (a) effective retention factors and enantioselectivity, and (b) eluent mobility (μ_{eo}). SA: (*R,S*)-Fmoc-Leu. EOF marker: acetone. Experimental conditions: stationary phase: CSP B; mobile phase: ACN–MES buffer (80:20); $\text{pH}_a=6$, adjusted with NEt_3 ; T : 20°C; voltage: –15 kV; injection: –15 kV/10 s; detection: UV at 250 nm.

clines in the following order: phosphate>acetate>MES>MES–HEPES. Generally, phosphate buffer yielded quite good peak efficiencies and the shortest run times. Unfortunately, under these conditions the electric current was unstable. Good results and stable currents could be obtained with MES and acetate buffers.

From Fig. 8 it can be seen that also the co-ion has a significant effect on the separations, in particular efficiencies are strongly affected (see Fig. 8). Theoretical plate numbers increased in the order ammonium<sodium<triethylammonium. Also some tetraalkylammonium ions have been tested, however,

without success. Briefly summarizing, with tetrabutylammonium and cetyltrimethylammonium as co-ions either of the two peaks of the corresponding enantiomers could be improved in symmetry and efficiency, while in most cases the efficiency of the other peak was deteriorated, in some cases showing peak distortion and peak splitting.

3.6. Influence of electric field strengths and linear flow-rates

As expected, with increasing electric field strengths linear flow-rates increase (see Fig. 9a and

Table 2
CEC data of the enantioseparation of DNZ-Leu on WAX type CSP B with different types of buffer^a

Buffer	μA	t_0 (min)	$k_{eff}(R)$	$k_{eff}(S)$	α	R_s	$N(R)$	$N(S)$
25 mM NaH_2PO_4 ($\text{pH}_a=5.8$)	–3.9 (c.i.) ^b	7.40	0.93	2.69	2.89	16.88	12 124	11 397
0.1 M MES–0.1 M HEPES (50:50) ($\text{pH}_a=6.0$; NEt_3)	–4.1	5.03	3.99	9.02	2.26	9.04	4234	2483
0.1 M MES–20 mM NaH_2PO_4 (50:50) ($\text{pH}_a=6.1$; NEt_3)	–5.4	6.72	1.69	4.12	2.43	13.2	7305	7170
0.1 M MES ($\text{pH}_a=6.1$; NEt_3)	–6.7	6.16	2.44	5.91	2.42	12.8	13 441	4277
0.1 M AcOH ($\text{pH}_a=6.1$; NEt_3)	–4.4	5.28	2.53	5.64	2.22	12.4	19 665	4442

^a Experimental conditions: mobile phase: ACN–buffer (80:20, v/v), voltage: –15 kV; injection: –15 kV/10 s; T : 20°C.

^b c.i.: Current instabilities.

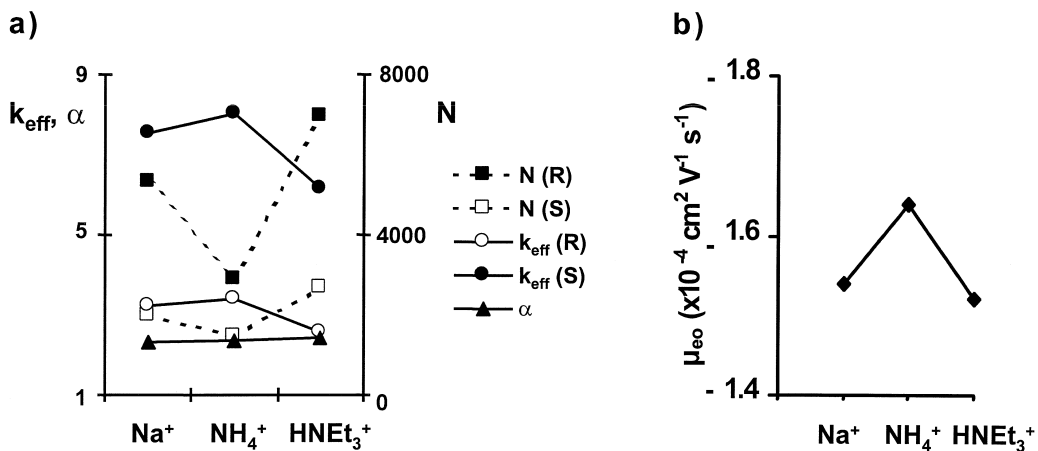


Fig. 8. Effect of co-ion on (a) the chromatographic parameters and (b) electroosmotic mobility (μ_{eo}). SA: racemic-DNZ-Leu. EOF marker: acetone. Experimental conditions: stationary phase: CSP B; mobile phase: ACN–0.1 M MES (80:20) ($\text{pH}_a=6.1$ adjusted either with NaOH, NH₃ or NEt₃); T : 20°C; voltage: –15 kV; injection: –15 kV/10 s; detection: UV at 250 nm.

b). Somewhat surprisingly, capillaries packed with CSP B and open bare fused-silica tubes (OT) exhibited similar linear flow-rates in magnitude (as

can be seen from Fig. 9b). On the other hand, non-porous CSP C generates much lower flow-rates. As already discussed, in any case linear flow-rates

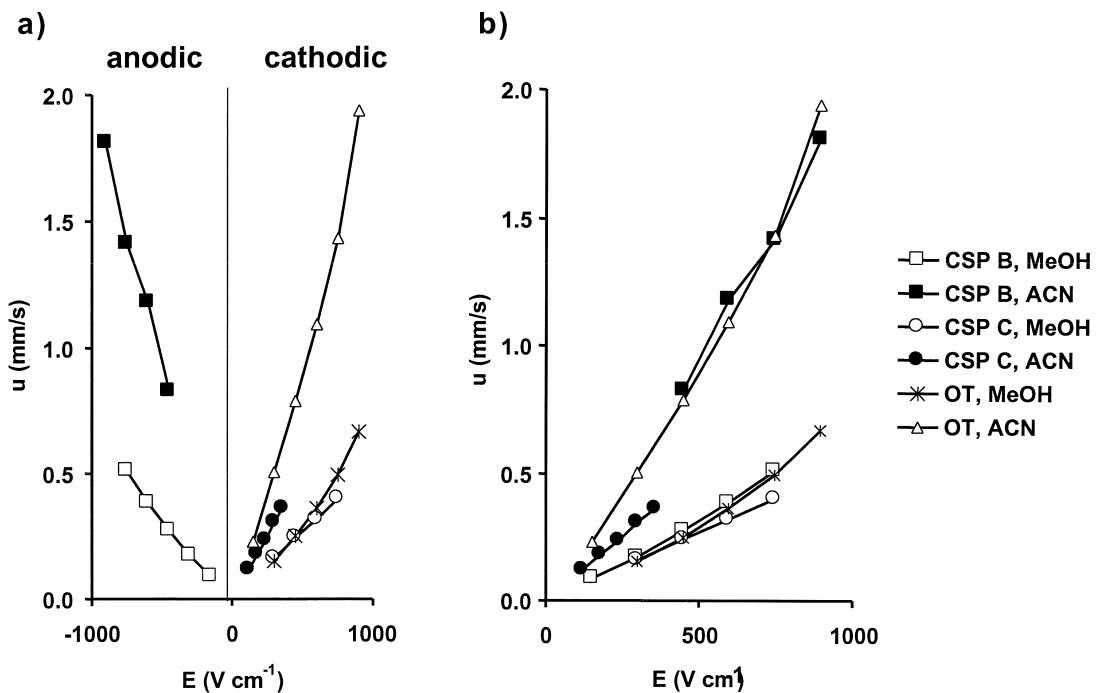


Fig. 9. Linear flow-rates in dependence of the applied electric field strength on CSPs B and C as well as in an open bare fused-silica capillary tube. EOF marker: acetone. Experimental conditions: mobile phase: organic modifier–0.1 M MES (80:20) ($\text{pH}_a=6.0$, adjusted with NEt₃); T : 20°C; injection: ± 5 kV/5 s; detection: UV at 250 nm.

were higher with acetonitrile than with methanol (see Fig. 9a and b).

The effect of linear flow velocities on efficiency is depicted in Fig. 10 by van Deemter plots. The shape of the van Deemter curves (H/u curves) obtained in CEC with the chiral anion exchangers under study

(CSPs B and C) deviates significantly from those usually observed in reversed-phase CEC of uncharged analytes. Flat H/u curves and minima at flow-rates around 1 mm/s or even higher are typical for the latter mentioned separation system [31,32], therefore recommending operation at high electric

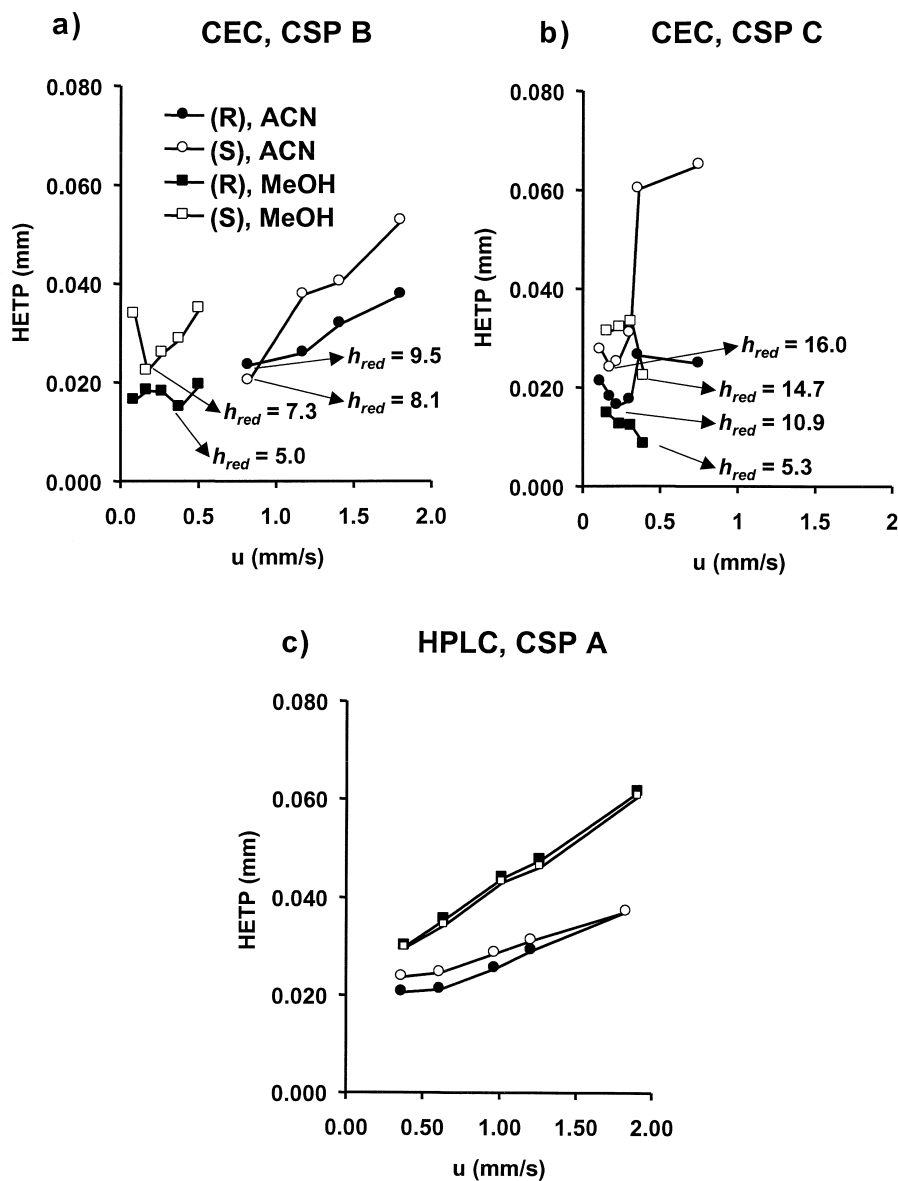


Fig. 10. Influence of linear flow-rates on theoretical plate heights (HETPs): (a) of (*R,S*)-Fmoc-Leu in CEC on CSP B, (b) of (*R,S*)-DNB-Leu in CEC on CSP C, and (c) of (*R,S*)-Fmoc-Leu in HPLC on CSP A. Experimental conditions: mobile phase: organic modifier–0.1 M MES (80:20) ($pH_a=6.0$, adjusted with NEt_3); T : 20°C; injection: CEC: –15 kV/10 s; HPLC: 20 μ l; detection: UV at 250 nm.

field strengths. In contrast, a significant C term in anion-exchange CEC enantioseparation of Fmoc-Leu with porous CSP B (anodic EOF, i.e., co-electrophoretic elution) contributes extraordinarily to peak broadening at higher electric field strengths and linear flow-rates. This can be largely explained by slow mass-transfer kinetics of the high affinity type anion-exchange process. The minima are located at linear flow-rates below 1 mm/s. Near the minimum plate heights of about 15 μm (MeOH) and 23 μm (ACN), respectively, for the less strong retained (R)-enantiomer and 22 μm (MeOH) and 20 μm (ACN), respectively, for the stronger retained (S)-enantiomer have been obtained at a capillary temperature of 20°C; this corresponds to reduced plate heights between 5 and 10 (see Fig. 12a). Regarding enantioseparation of DNB-Leu on CSP C, with acetonitrile as organic modifier (cathodic EOF and electroosmotically dominated elution mode), the C term is even more significant and the minima are located at flow-rates between 0.2 and 0.3 mm/s. Minimum plate heights of 16 μm ($h_{\text{red}}=11$) for the (R)-enantiomer and 24 μm ($h_{\text{red}}=16$) for the (S)-enantiomer have been calculated. On the other side, the H/u curves obtained with methanol (cathodic

EOF and electrophoretically dominated elution, i.e., EOF directed to the injection end of the capillary) exhibit a different characteristics reflecting the significance of the electrophoretic process. With increasing flow velocities (equivalent to increasing electric field strengths) plate heights of the less retained (R)-enantiomer decrease (a relative minimum is obtained at a flow-rate of 0.4 mm/s or –25 kV with a plate height of 8 μm or a reduced plate height of 5.3). Plate heights of the stronger adsorbed (S)-enantiomer, however, are by a factor of about 3 higher (22 μm minimum plate height or a reduced plate height of 14.7). For comparison, H/u curves obtained by HPLC on CSP A are shown in Fig. 10c). Overall, the presented H/u curves for the different modes of elution and the corresponding reduced plate heights at the minima suggest that the co-electrophoretic elution mode is preferred also with respect to efficiency.

3.7. Influence of capillary temperature

H/u dependencies of Fmoc-Leu enantiomers on CSP B have also been studied for different capillary temperatures (see Fig. 11a). As expected, plate

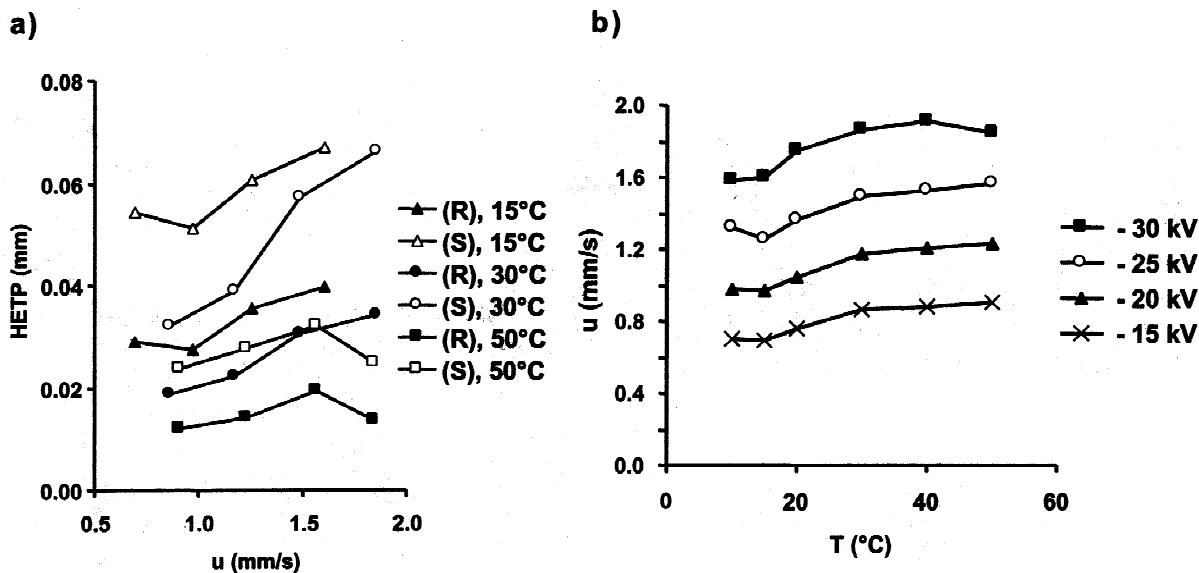


Fig. 11. Temperature dependence of (a) H/u curves, and (b) linear flow-rates on CSP B. SA: (R,S)-Fmoc-Leu. EOF marker: acetone. Experimental conditions: mobile phase: ACN–0.1 M MES (80:20) ($\text{pH}_a=6.0$, adjusted with NEt_3); injection: –15 kV/10 s (SA) and –5 kV/5 s (acetone); detection: UV at 250 nm.

heights decreased with increasing temperature and due to a faster mass transfer kinetics at higher temperatures H/u curves become flatter, favorable for operation at higher electric field strengths. Simultaneously, slightly enhanced EOF velocities at elevated temperatures (see Fig. 11b) and decreased retention factors yield faster elution and shorter run times. This leads to a considerable improvement of the separations as depicted in Fig. 12.

3.8. Repeatability

In order to get some information about the reliability of the proposed separation methods involving ionic interactions between oppositely charged

analytes and anion-exchange type chiral sorbent, a repeatability study has been carried out injecting 10 times the same sample (racemic-DNB-Leu) onto CSP C without renewing the mobile phase during the 10 consecutive injections. The results are summarized in Table 3. Void times t_0 (acetone), retention times of (*R*)- and (*S*)-enantiomers, as well as enantioselectivity values could be reproduced with relative standard deviations (RSDs) below 2%. This compares rather well with reversed-phase type CEC separations. The electric current constantly slightly decreased from run to run; this observation has been attributed to buffer depletion. For effective retention factors, resolution and theoretical plate numbers RSD values between 4 and 9% have been calculated.

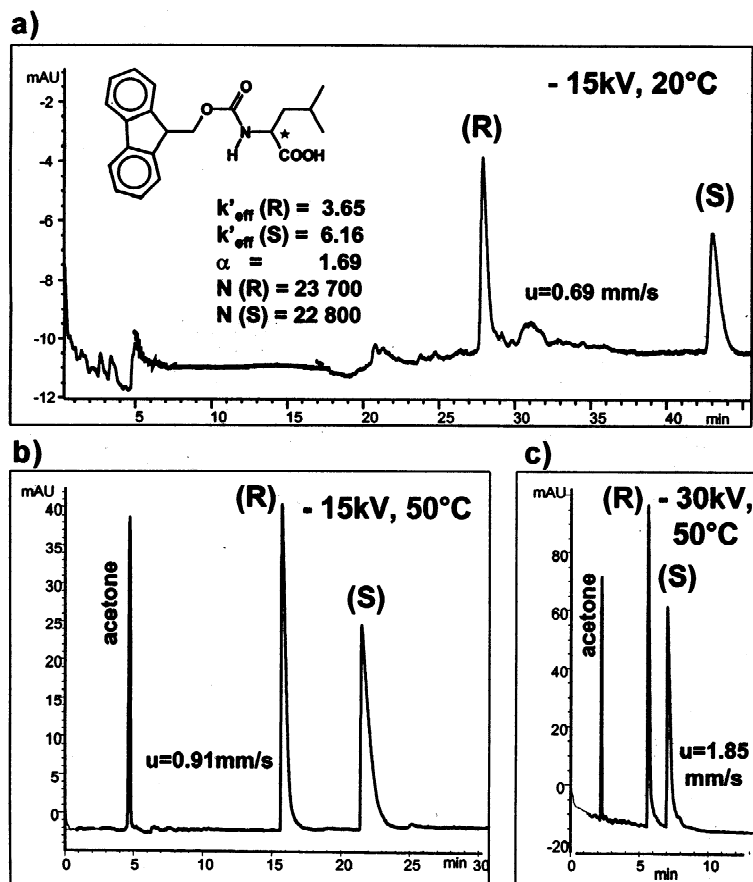


Fig. 12. CEC enantioseparation of (*R,S*)-Fmoc-Leu on CSP B as function of temperature and applied voltage. (a) -15 kV, 20°C; (b) -15 kV, 50°C; (c) -30 kV, 50°C. Experimental conditions: mobile phase: ACN-0.1 M MES (80:20) ($\text{pH}_a = 6.2$; NEt_3); injection: -15 kV/30 s; detection: UV at 250 nm.

Table 3
Repeatability study (sample: DNB-Leu; $n=10$)^a

	I (μ A)	t_0 (acetone) (min)	t_R (R) (min)	t_R (S) (min)	k_{eff} (R)	k_{eff} (S)	α	R_S	N (R)	N (S)	Area (R)	Area (S)	Area % (R)	Area % (S)
Mean	0.37	23.64	34.05	36.06	0.44	0.53	1.19	1.37	11 051	7732	308.5	337.3	47.6	52.4
RSD (%)	2.5	0.6	1.4	1.6	4.4	4.6	0.5	5.5	8.5	7.3	43.1	41.4	1.4	1.2
Minimum	0.35	23.47	33.27	35.13	0.41	0.49	1.18	1.26	9562	6942	159.6	174.3	46.9	51.3
Maximum	0.38	23.98	34.89	37.09	0.47	0.57	1.2	1.49	12 601	8615	581.2	615.3	48.7	53.2

^a Experimental conditions: stationary phase: CSP C; mobile phase: ACN–0.1 M MES (80:20) ($\text{pH}_a=5.0$; NEt_3); T : 20°C; voltage: +6 kV; injection: +10 kV/5 s; detection: UV at 250 nm.

This is satisfactory, especially if compared with the run-to-run repeatabilities of plate numbers observed for basic compounds on cation exchangers which were found to be poorly reproducible due to zone focusing effects. On the other hand, area repeatability (ca. 40%) is very poor. For practical applications and the determination of the enantiomeric composition of a sample, relative peak areas are commonly used, for which good RSD values have been obtained (1.4 and 1.2%), providing reliable results.

4. Conclusions

It could be shown that chiral anion exchangers developed for HPLC enantioseparation of chiral acids can also be applied to CEC, as they are optimally compatible to CEC owing to their preferred aqueous–organic operation mode. If silica is used as chromatographic support material for immobilization of the positively charged chiral selectors, the surface of the chiral anion exchanger has quasi “zwitterionic” character, allowing cathodic as well as anodic EOF depending on the mobile phase pH and the apparent pI of the surface. Accordingly, selection of the type of silica is critical, as it determines the pI . At pH values above the apparent pI of the CSPs cathodic flow and below the pI anodic EOF was observed. The latter mode of operation seems to be preferred for the analysis of negatively charged solutes with respect to run times and also efficiency. Slow ion-exchange kinetics of this affinity type chromatographic system contributes significantly to peak broadening at higher electric field strengths so that linear flow-rates yielding minimum plate heights are typically found below 0.5 mm/s. Concomitantly, this leads to long run times

due to the strong ionic interactions which are more difficult to balance than in HPLC. On the other hand, shorter columns and/or macroporous support materials, which are supposed to yield higher flow-rates due to favorable intrapore flow and flatter H/u curves, might be possible solutions to the problem of long run times.

Acknowledgements

F.Th. Hafner of the research group of Professor H. Engelhardt from the University of Saarland, Saarbrücken, Germany and C. Yan (Unimicro Technologies, Pleasanton, CA, USA) are acknowledged for packing capillary columns. We would like to thank also Hewlett-Packard (Vienna, Austria) for their generous installation of a CEC instrument for an extensive period of time to carry out the presented studies.

References

- [1] F. Lelievre, C. Yan, R.N. Zare, P. Gareil, J. Chromatogr. A 723 (1996) 145.
- [2] Y.L. Deng, J.H. Zhang, T. Tsuda, P.H. Yu, A.A. Boulton, R.M. Cassidy, Anal. Chem. 70 (1998) 4586.
- [3] M.K. Ho, S.J. Wang, M.D. Porter, Anal. Chem. 70 (1998) 4314.
- [4] S. Wang, M.D. Porter, J. Chromatogr. A 828 (1998) 157.
- [5] W. Wei, G.A. Luo, R. Xiang, C. Yan, J. Microcol. Sep. 11 (1999) 263.
- [6] M. Lämmerhofer, W. Lindner, J. Chromatogr. A 839 (1999) 167.
- [7] S. Li, D.K. Lloyd, Anal. Chem. 65 (1993) 3684.
- [8] D.K. Lloyd, S. Li, P. Ryan, J. Chromatogr. A 694 (1995) 285.
- [9] S. Li, D.K. Lloyd, J. Chromatogr. A 666 (1994) 321.

- [10] D. Wistuba, H. Czesla, M. Roeder, V. Schurig, J. Chromatogr. A 815 (1998) 183.
- [11] C. Wolf, P.L. Spence, W.H. Pirkle, E.M. Derrico, D.M. Cavender, G.P. Rozing, J. Chromatogr. A 782 (1997) 175.
- [12] A. Dermaux, F. Lynen, P. Sandra, J. High Resolut. Chromatogr. 21 (1998) 575.
- [13] K. Krause, M. Girod, B. Chankvetadze, G. Blaschke, J. Chromatogr. A 837 (1999) 51.
- [14] J.-M. Lin, T. Nakagama, K. Uchiyama, T. Hobo, Biomed. Chromatogr. 11 (1997) 298.
- [15] J.-M. Lin, K. Uchiyama, T. Hobo, Chromatographia 47 (1998) 625.
- [16] L. Schweitz, L.I. Andersson, S. Nilsson, Anal. Chem. 69 (1997) 1179.
- [17] L. Schweitz, L.I. Andersson, S. Nilsson, J. Chromatogr. A 817 (1998) 5.
- [18] E.C. Peters, K. Lewandowski, M. Petro, F. Svec, J.M.J. Frechet, Anal. Commun. 35 (1998) 83.
- [19] M. Lämmerhofer, W. Lindner, J. Chromatogr. A 829 (1998) 115.
- [20] M. Lämmerhofer, N.M. Maier, W. Lindner, Am. Lab. 30 (1998) 71.
- [21] A. Mandl, L. Nicoletti, M. Lämmerhofer, W. Lindner, J. Chromatogr. A 858 (1999) 1.
- [22] M. Lämmerhofer, W. Lindner, GIT Special – Chromatogr. Int. 96 (1996) 16.
- [23] V. Piette, M. Lämmerhofer, K. Bischoff, W. Lindner, Chirality 9 (1997) 157.
- [24] M. Lämmerhofer, W. Lindner, J. Chromatogr. A 741 (1996) 33.
- [25] N.M. Maier, L. Nicoletti, M. Lämmerhofer, W. Lindner, Chirality 11 (1999) 522.
- [26] J. Lesnik, M. Lämmerhofer, W. Lindner, Anal. Chim. Acta 401 (1999) 3.
- [27] W. Lindner, M. Lämmerhofer, N.M. Maier, European Patent Application PCT/EP97/02888 (1997).
- [28] O.P. Kleidernigg, M. Lämmerhofer, W. Lindner, Enantiomer 1 (1996) 387.
- [29] H. Rebscher, U. Pyell, Chromatographia 38 (1994) 737.
- [30] M.M. Dittmann, G.P. Rozing, J. Microcol. Sep. 5 (1997) 399.
- [31] R.M. Seifar, S. Heemstar, W.T. Kok, J.C. Kraak, H. Poppe, J. Microcol. Sep. 10 (1998) 41.
- [32] R.M. Seifar, W.T. Kok, J.C. Kraak, H. Poppe, Chromatographia 46 (1997) 131.